Atmos. Chem. Phys. Discuss., 14, 13731–13767, 2014
www.atmos-chem-phys-discuss.net/14/13731/2014/
doi:10.5194/acpd-14-13731-2014

Atmospheric Chemistry and Physics Discussions

The effect of dry and wet deposition of condensable vapors on secondary organic aerosols concentrations over the continental US

C. Knote[1], A. Hodzic[1], and J. L. Jimenez[2]

[1]Atmospheric Chemistry Division, NCAR, Boulder, CO, USA
[2]Department of Chemistry and Biochemistry, University of Colorado at Boulder, CO, USA

Received: 10 May 2014 – Accepted: 14 May 2014 – Published: 26 May 2014

Correspondence to: A. Hodzic (alma@ucar.edu)

Published by Copernicus Publications on behalf of the European Geosciences Union.

Abstract

The effect of dry and wet deposition of semi-volatile organic compounds (SVOC) in the gas-phase on the concentrations of secondary organic aerosol (SOA) is reassessed using recently derived water solubility information. The water solubility of SVOCs was implemented as a function of their volatility distribution within the regional chemistry transport model WRF-Chem, and simulations were carried out over the continental United States for the year 2010. Results show that including dry and wet removal of gas-phase SVOCs reduces annual average surface concentrations of anthropogenic and biogenic SOA by 48 % and 63 % respectively over the continental US Dry deposition of gas-phase SVOCs is found to be more effective than wet deposition in reducing SOA concentrations (−40 % vs. −8 % for anthropogenics, −52 % vs. −11 % for biogenics). Reductions for biogenic SOA are found to be higher due to the higher water solubility of biogenic SVOCs. The majority of the total mass of SVOC + SOA is actually deposited via the gas-phase (61 % for anthropogenics, 76 % for biogenics). A number of sensitivity studies shows that this is a robust feature of the modeling system. Other models that do not consider dry and wet removal of gas-phase SVOCs would hence overestimate SOA concentrations by roughly 50 %. Assumptions about the water solubility of SVOCs made in some current modeling systems ($H^* = 10^5\,\mathrm{M\,atm^{-1}}$; $H^* = H^*(\mathrm{HNO_3})$) still lead to an overestimation of 25 %/10 % compared to our best estimate. A saturation effect is observed for Henry's law constants above $10^8\,\mathrm{M\,atm^{-1}}$, suggesting an upper bound of reductions in surface level SOA concentrations by 60 % through removal of gas-phase SVOCs. Considering reactivity of gas-phase SVOCs in the dry deposition scheme was found to be negligible. Further sensitivity studies where we reduce the volatility of organic matter show that consideration of gas-phase SVOC removal still reduces average SOA concentrations by 31 % on average. We consider this a lower bound for the effect of gas-phase SVOC removal on SOA concentrations.

ACPD
14, 13731–13767, 2014

1 Introduction

Organic compounds represent a major, often dominant mass fraction of ambient aerosol (e.g. Murphy et al., 2006; Jimenez et al., 2009). Most of this mass results from the multigenerational oxidation of hydrocarbons forming products with lower volatility (Odum et al., 1996; Jimenez et al., 2009). The resulting oxygenated semivolatile organic compounds (SVOCs) equilibrate between the gas- and the particle-phase according to their saturation vapor pressure C^* ($\mu g\,m^{-3}$, Pankow, 1994). Under ambient conditions in the troposphere, SVOCs with a C^* below $0.1\,\mu g\,m^{-3}$ are predominantly found in the particle-phase, while products with saturation vapor pressure C^* between 0.1 and $10^3\,\mu g\,m^{-3}$, are distributed between the gas- and the particle-phase with significant mass fractions in both phases. Aerosol volatility measurements during the MILAGRO campaign in Mexico City and similar observations for the Los Angeles area (Cappa and Jimenez, 2010) estimated that for organic material with $C^* \leq 10^3\,\mu g\,m^{-3}$ the total amount in the gas-phase is between 0.7 to 2.4 times that of the mass in the particle-phase. Recent findings from explicit oxidation chemistry modeling (Hodzic et al., 2013, 2014a) with the Generator of Explicit Chemistry and Kinetics of Organics in the Atmosphere (GECKO-A Aumont et al., 2005) together with structure-activity estimation of solubility (Raventos-Duran et al., 2010) suggests that many SVOCs are highly water soluble, with Henry's law constants H^* between 10^5 and $10^{10}\,M\,atm^{-1}$. This makes them very susceptible to removal processes in the atmosphere (wet deposition and dry deposition to wet surfaces/vegetation). Given that gas- and particle-phase are in equilibrium, this also implies that removal of gas-phase SVOCs could be an important indirect sink of SOA mass.

Currently, the removal of organic aerosols in 3-D models relies for the main part on wet deposition of aerosols (Tsigaridis et al., 2014) and the model's ability to accurately predict clouds and precipitation. Dry deposition of aerosols is a small contributor to this removal. Deposition of gas-phase SVOCs in current modeling systems is largely unconstrained and, if considered at all, typically scaled to the deposition of

ACPD
14, 13731–13767, 2014

HNO_3 as a very soluble reference compound. Bessagnet et al. (2010) investigated the effect of dry deposition of gas-phase SVOCs on SOA concentrations over Europe. In their simulations they used Henry's law constants from different reference compounds (with H^* ranging from 10^5 to 10^{16} M atm^{-1}) and found that SOA concentrations are reduced by 20 to 30 % when including dry deposition of gas-phase SVOCs, mostly due to the removal of biogenic SVOCs. Pye and Seinfeld (2010) applied the global GEOS-chem model to look at the SOA formation from low volatile compounds. For SVOCs, they distinguished between freshly emitted ones with a very low Henry's law constant (< 10 M atm^{-1}) and oxidation products that are treated using a Henry's law constant of 10^5 M atm^{-1}. They found that a considerable fraction is removed through the gas-phase, and that wet deposition dominates the removal pathways. In a sensitivity study they lowered the Henry's law constants for SVOCs and showed that the global OA budget is sensitive to this parameter, but they concluded that this does not decrease the model bias against observations. Ahmadov et al. (2012) implemented a VBS model into WRF-Chem and found that SOA concentrations are very sensitive to the assumptions made on dry deposition of gas-phase SVOCs. They did not include wet deposition, and tentatively suggested to dry deposit SVOCs in the gas-phase 0.25 to 0.5 times the rate of HNO_3 to optimize the agreement with observations. These studies show that treatment of gas-phase SVOC removal can significantly affect our ability to accurately predict SOA concentrations. Recently, Hodzic et al. (2014a) have provided a parameterization of the water solubility of SVOCs based on explicit oxidation chemistry modeling combined with estimation of Henry's law constants that is constrained from experimental data. Their results show that SVOC mixtures typically created through oxidation in the atmosphere are highly water soluble, 2–3 orders of magnitude higher that e.g. assumed in Pye and Seinfeld (2010). No previous study investigated the combined effect of dry as well as wet deposition of SVOCs in the gas-phase with such high values for water solubility.

In this work we have integrated the new findings of Hodzic et al. (2014a) regarding the solubility of SVOCs into a state-of-the-art online modeling system (WRF-Chem)

ACPD
14, 13731–13767, 2014

and perform a detailed assessment of the effects of the gas-phase SVOC wet and dry deposition on predicted SOA concentrations over North America. We implement a volatility basis set (VBS) scheme with 5 volatility bins in our configuration of WRF-Chem based the work of Lane et al. (2008b) and Ahmadov et al. (2012) to consider the formation of compounds with lower volatility and their partitioning between gas- and aerosol phase. The dry and wet deposition schemes in WRF-Chem are extended to consider removal of gas-phase SVOCs based on their estimated Henry's law constants for each volatility bin. Simulations are performed for the full year of 2010 to understand the impact of these removal processes under very different ambient conditions, and test their robustness within the model parameter space.

In Sect. 2 we present the modeling approach. Section 3 deals with the evaluation of model performance in terms of precipitation and removal of inorganic substances. Finally, in Sect. 4, we address the effects of dry/wet removal of gas-phase SVOCs on SOA concentrations.

2 Modeling

WRF-Chem v3.5 is used for all simulations. Meteorological processes and their parameterizations chosen for our simulations are summarized in Table 1.

The MOZART-4 gas-phase mechanism (Emmons et al., 2010) with more explicit treatment of aromatic compounds (Knote et al., 2013) and monoterpenes (Hodzic et al., 2014b) is used together with the MOSAIC 4-bin aerosol module (Zaveri et al., 2008).

2.1 The volatility basis set

MOSAIC has been extended by a volatility basis set parameterization to describe SOA formation based on the work of Lane et al. (2008a, b) and (Ahmadov et al., 2012). In Fig. 1 we present a schematic overview of the new module. Five volatility bins are considered (saturation concentrations C^* of 0.001, 1, 10, 100 and 1000 $\mu g\,m^{-3}$ at 298 K)

ACPD
14, 13731–13767, 2014

for both anthropogenic and biogenic precursors (see Table S1 for mapping SAPRC99 species to MOZART). The lowest volatility bin (C^* of 0.001 µg m^{-3}) has been added to avoid an unrealistically volatile mixture after substantial aging. We consider different SOA yields for low and high NO_x conditions, and the branching ratio B to determine the respective contributions is calculated according to Lane et al. (2008a) as

$$\beta = k_{(RO_2+NO)}[NO]/(k_{(RO_2+NO)}[NO] + k_{(RO_2+HO_2)}[HO_2]) \quad (1)$$

with $k_{(RO_2+NO)}$ and $k_{(RO_2+HO_2)}$ the reaction rate constants for the reaction of an organic peroxy radical (RO_2) with NO vs. its reaction with HO_2 respectively. OH and O_3 act as oxidizing agents. To reduce the computational burden we sum up all mass formed from anthropogenic and biogenic precursors respectively and only keep track of total anthropogenic and total biogenic SVOC/SOA mass (called aSVOC/bSVOC and aSOA/bSOA in the following). Pseudo-ideal partitioning theory based on Pankow (1994) is used to estimate gas-aerosol partitioning as implemented in MOSAIC by Shrivastava et al. (2011). Values for the enthalpy of vaporization (ΔH) for each bin have been derived using the semi-empirical parameterization of Epstein et al. (2009) leading to values between 100 and 140 kJ mol^{-1} for the bins with C^* of 1, 10, 100, and 1000 µg m^{-3} (see Fig. 1 for exact values). The lowest volatility bin uses a ΔH of 40 kJ mol^{-1}. "Aging" of condensable vapors through OH oxidation (mass transfer into the next lower volatility bin) is done with a fixed rate of 1.0×10^{-11} cm^3 molec^{-1} s^{-1} (Murphy and Pandis, 2009), and a 7.5 % mass increase due to the addition of oxygen atoms (e.g. Ahmadov et al., 2012). Secondary aerosol mass formed is assumed to have a density of 1.5 g m^{-3} (Lane et al., 2008a) and a molecular weight of 250 g mol^{-1}. Direct emissions of organic particulates (primary organic aerosols, POA) are included as inert contribution to organic aerosol mass without consideration of evaporation and re-condensation.

2.2 Dry and wet deposition of gases and aerosols

Washout of gases and aerosols by convective precipitation is considered using the scheme included in WRF-Chem (based on Grell and Dévényi, 2002) which we mod-

ACPD
14, 13731–13767, 2014

ified to use Henry's law constants in gas-droplet partitioning. Grid-scale precipitation removes aerosols through the scheme implemented in MOSAIC (Easter et al., 2004; Chapman et al., 2009), while washout of trace gases is performed as described in (Neu and Prather, 2012). The Neu and Prather (2012) scheme also employs an equilibrium approach based on Henry's law constants to consider transfer into cloud droplets and subsequent conversion into rain droplets, as well as collection of gases by falling rain droplets. Both, washout through grid-scale and convective precipitation considers the same set of gas species with an identical set of Henry's law constants. Dry deposition of gases is parameterized in WRF-Chem based on Wesely (1989), modeling deposition as a series of resistors consisting of an atmospheric, a laminar sublayer, and a bulk surface resistance. The latter is a function of the Henry's law constant of a gas to describe partitioning into plants and other wet surfaces. A reactivity factor f_0 (ranging from $f_0 = 0$ for non-reactive species to $f_0 = 1$ for species as reactive as O_3) is used in this scheme to consider oxidation of biological substances within plants once a species partitions into this volume. This is set to 0.0 for SVOCs. Hodzic et al. (2014a) presented Henry's law constants (H^*, M atm^{-1}) for semi-volatile oxidation products created from different anthropogenic and biogenic SOA precursors including alkanes, aromatics, or isoprene and terpenes which they derived from explicit oxidation chemistry simulations using the GECKO-A model (Aumont et al., 2005). They also derived a parameterization of H^* as a function of precursor and saturation vapor pressure (C^*). In the VBS only total anthropogenic and biogenic SVOC mass is tracked – precursor information is lost. We hence calculated unweighted averages of H^* of the anthropogenic and biogenic precursors considered in the VBS parameterization to derive a value of H^* for anthropogenic and biogenic SVOCs in each volatility bin (Table 2). Dry and/or wet deposition of these volatile compounds is then considered by adding these species to the respective modules in WRF-Chem described above.

ACPD
14, 13731–13767, 2014

2.3 Model setup

Simulations were set up to cover the continental US at 36 km horizontal resolution and 33 levels up to 50 hPa. Meteorological parameters are initialized and forced at the boundaries by 6 hourly analyses (interlaced with 3 hourly forecasts) of the Global Forecasting System (GFS) of the National Center for Environmental Prediction (National Centers for Environmental Prediction/National Weather Service/NOAA/US Department of Commerce, 2010). Initial and boundary conditions for chemistry are provided by simulations of the IFS-MOZART global chemistry transport model (Stein et al., 2012) conducted within the MACC project. Emissions of trace gases and aerosols are based on the US Environmental Protection Agency (US EPA) National Emission Inventory (NEI) updated for the year 2010 within the Air Quality Model Evaluation International Initiative (AQMEII Rao et al., 2011) model intercomparison (phase 2). The simulations are split into 48 h long chunks of free running meteorology (only forced at the boundaries) without nudging. Each of these runs is preceded by a 6 h meteorology-only spin up started from GFS analyses and nudged to the forcing data above the planetary boundary layer. Concentrations fields for trace gases and aerosol quantities resulting from the previous run are then used to initialize the following free run. Thereby, meteorology is restarted from analyses every 48 h, while chemistry is continuous over the whole period. All simulations have been conducted on NCAR's Yellowstone computing system (Computational and Information Systems Laboratory, 2012).

Table 3 lists all simulations conducted. In a first simulation (NODEP) we ignore both dry and wet deposition of SVOCs. In further three simulations we consider dry, wet, and dry + wet deposition of SVOCs (called DRY, WET and REF respectively) employing Henry's law values calculated by Hodzic et al. (2014a). The simulation with dry and wet deposition of SVOCs according to Hodzic et al. (2014a) is our best estimate and hence called REF. All these simulations were carried out for the full year 2010 with an additional 1 week of spin-up for chemistry (not used in the analysis). A number of sensitivity studies were conducted to understand the sensitivity of the predictions

ACPD
14, 13731–13767, 2014

to uncertainties in the process parameterizations. In LOWVOL and FAST_AGING we vary the SOA formation mechanism. In LOWVOL we decrease the overall volatility of the SOA formed by increasing the rate of aging from the volatility bin at $C^* = 1\,\mu g\,m^{-3}$ to the one with $C^* = 0.001\,\mu g\,m^{-3}$ by a factor of 10, thereby moving aged SOA to a bin with negligible partitioning into the gas-phase and hence leaving less SVOC that would be susceptible to the newly included removal processes. In FAST_AGING we increase the aging rate constants for all volatility bins to $4.0 \times 10^{-11}\,cm^3\,molec^{-1}\,s^{-1}$, thereby matching assumptions about the rate of aging used in previous modeling studies (e.g. Athanasopoulou et al., 2013), and again decreasing the amount of SVOC available for removal. Four additional simulations were conducted to determine the model sensitivity to assumptions about the Henry's law constants of SVOCs and identify a possible saturation effect at very high H^* values in the dry deposition scheme. The Wesely (1989) scheme used represents dry deposition as a series of resistances, with only the land surface/canopy resistance being affected by changes in H^*. At very high H^*, this resistance should become negligible and dry deposition would be governed by the remaining resistances. In H_1E5, H_1E8 and H_1E10 we employ Henry's law constants for SVOCs of 10^5, 10^8, and $10^{10}\,M\,atm^{-1}$ respectively in both dry and wet deposition. The fourth simulation (H_HNO3) uses the Henry's law constant of HNO_3 for SVOCs. The solubility of HNO_3 (or a fraction of it) is often used in atmospheric modeling to treat compounds with unknown properties, but which are assumed to be very soluble. In the final two simulations (F_0.1 and F_1.0) we investigate the effect of the reactivity factor f_0 on predictions. Which SVOCs should be considered "reactive" is so far poorly constrained, but Karl et al. (2010) suggested that assuming $f_0 = 0.1$ or 0.0 as it is typically done for NMVOCs in current modeling systems might be too low. We vary it here to $f_0 = 0.1$ (F_0.1) and $f_0 = 1.0$ (F_1.0). All these sensitivity studies were conducted for the months of June, July and August of 2010 only.

ACPD
14, 13731–13767, 2014

3 Evaluation of predicted wet deposition

An accurate description of the spatiotemporal variability of precipitation is a prerequisite for modeling (wet) deposition. In Fig. 2 we compare our simulations against a composite of rain gauge and radar observations from the National Weather Service River Forecast Centers (http://water.weather.gov/precip/download.php) which provides daily accumulated precipitation amounts. Apart from a tendency of the model to overestimate rainfall amounts in the rather dry regions of the western United States the differences in the yearly accumulated precipitation are typically below ±25 %.

Wet deposition measurements from the National Atmospheric Deposition Program (NADP, http://nadp.sws.uiuc.edu) are used to evaluate wet deposition of inorganic compounds (SO_4^{2-}, NO_3^-, NH_4^+). In Fig. 3 we compare monthly accumulated deposition of sulfate, nitrate and ammonium and find good agreement between model and measurements for sulfate (Pearson's correlation coefficient squared $R^2 = 0.62$, normalized mean bias NMB = 3 %) and nitrate ($R^2 = 0.65$, NMB = 7 %), while the amount of wet deposition of ammonium is underestimated but still has a good correlation with measurements ($R^2 = 0.69$, NMB = 0.69). Measurements of water-soluble organics are not available so we could not directly evaluate the performance of WRF-Chem. The model results of wet deposition of inorganic ions however shows that the underlying processes are accurately modeled, lending credibility to the accuracy of the wet deposition of organic substances.

4 Effect of SVOC deposition on SOA concentrations

4.1 Effect on SOA concentrations

We first evaluate the differences in the average concentrations of SOA due to the removal of SVOCs. Dry deposition has a much stronger effect on SOA concentrations at the surface (top right map in Fig. 4) than does wet deposition (Fig. 4, bottom right map).

ACPD
14, 13731–13767, 2014

As a yearly average over the continental US, dry deposition of SVOCs reduces SOA surface level concentrations by 46 % (aSOA: 40 %, bSOA: 52 %), whereas wet deposition leads to SOA concentrations at the surface that are lower by 10 % (aSOA: 8 %, bSOA: 11 %) vs. not considering this removal pathway (REF vs. NODEP cases). We find very similar results when analyzing changes averaged over the planetary boundary layer instead of changes in the surface layer. SOA seems to be most sensitive to dry removal of SVOCs over the Pacific Northwest coast, the northern Midwest (Montana, South/North Dakota) and parts of eastern Canada. Wet deposition is most effective around the Great Lakes area, and least effective over the Nevada/Utah/Arizona area as well as northeastern Texas. When looking at the average vertical profiles of SOA concentrations over land (Fig. 4, left panel) we find that the effects of these removal processes are visible throughout the vertical column. Dry deposition of SVOCs has the additional effect of removing a local maximum of SOA concentrations in the lowest model layers. When comparing the sum of the reductions due to only considering either dry (DRY) or wet (WET) deposition of SVOCs against the reductions in a simulation where we consider both processes (REF) we find that their effects are almost additive (not shown).

We evaluate the resulting total organic aerosol (OA) concentrations against measurements using measurements of the Interagency Monitoring of Protected Visual Environments network (IMPROVE, data hosted at http://www.epa.gov/ttn/airs/airsaqs/detaildata/downloadaqsdata.htm, accessed 6 February 2014). In Fig. 5 we show comparisons of organic carbon (OC) in particles below 2.5 µm in diameter. Modeled concentrations are the sum of aSOA, bSOA and POA converted from organic aerosol mass to organic carbon assuming OA/OC ratios of 2.0 for a/bSOA and 1.4 for POA (comparable to findings of Aiken et al., 2008). When comparing the results from the REF run where we consider both dry and wet deposition of SVOCs we find reasonable correlation ($R^2 = 0.58$) with measurements and an underestimation of the modeled amounts (NMB = −34 %). When analyzing the results from the simulation without SVOC removals (NODEP, middle plot) it is clear that the effect of these removals has

ACPD
14, 13731–13767, 2014

a pronounced annual cycle, being almost negligible in winter while reducing concentrations of secondary formed OC by half. It is important to note that very different types of biases are observed here between the run without SVOC removals and the one where these are included: annually averaged, the OC mass predicted in the NODEP simulation would match annual averaged measured concentrations well, but there is a distinctly different evolution over the course of the year – the simulation shows a much stronger annual amplitude in OC than observed, underestimating measured values in winter and strongly overestimating in summer. In the REF simulation with removals, the overall concentrations of OC are underestimated compared to measurements, but the annual evolution is considerably more similar to the observed evolution. In our study we only consider "traditional" SOA formation mechanisms (pure gas-phase oxidation), but a number of additional processes have been proposed (cloud-phase formation, e.g. Lim et al., 2010; in-aerosol formation, e.g. Knote et al., 2013; evaporation of primary OA, e.g. Robinson et al., 2007; additional formation pathways from existing precursors like isoprene, e.g. Paulot et al., 2009). Assuming that the products formed from these new sources will exhibit similar volatility/water solubility relationships than the existing compounds, the effect of SVOC removal will be similar. Including these processes would then lead to a general shift of the annual cycle of concentrations as shown in Fig. 5 towards higher values, potentially closing the gap between measurements and model results.

4.2 Total deposition for the different pathways

A comparison of the monthly and yearly accumulated deposition mass through the different removal pathways is shown in Fig. 6. We find that for the total of anthropogenic and especially for biogenic SVOC + SOA, more mass is removed as SVOCs (anthropogenics: 38.0 % via dry dep. and 24.2 % through wet dep. = 62.2 % total, biogenics: 54.1 % via dry dep. and 21.9 % through wet dep. = 76 % % total) than as particles (pie charts in the right column of Fig. 6). Dry deposition is the most efficient removal process for both types of organic species. Wet deposition of SVOCs and SOA is roughly

ACPD
14, 13731–13767, 2014

equivalent, dry deposition of particles is small (< 5 %). The annual cycle of monthly accumulated deposition (left column, Fig. 6) shows a more pronounced annual variability of biogenic deposition. In winter, deposition of biogenic SVOC and SOA is negligible (due to the very low biogenic emissions), whereas deposition of anthropogenic SVOC + SOA in winter months is still about a quarter of the deposition in the summer months.

5 Discussion of uncertainties

The results presented above are valid for our particular model configuration. We investigated the sensitivity of these results to the model parameter space, considering uncertainties in the SOA formation mechanisms as well as in the treatment of deposition.

5.1 Volatility of the secondary organic aerosol formed

How susceptible SOA is to the removal of SVOCs in the gas-phase depends on the overall partitioning between gas- and particle-phase. In two sensitivity studies we change SOA volatility to investigate the impact: in LOWVOL we increase the aging rate constant into very low-volatility SOA (kOH of volatility bin with $C^* = 1$ to the bin with $C^* = 10^{-4}$) by a factor of 10, effectively hiding aged organic material from gas-phase removal. In FAST_AGING we increase the aging rate constants between all volatility bins by a factor of 4, reducing the time organic material is exposed to gas-phase removal during aging. Both changes result in a much less volatile distribution of mass which is less susceptible to gas-phase removals. The reader is referred to the Appendix for a box model study on the effects of these changes. The resulting volatility distributions are comparable to what has been observed in the atmosphere (Cappa and Jimenez, 2010), hence we deem this to be a lower bound of the effect of gas-phase removal on SOA concentrations. As expected, we find (Ta-

ACPD
14, 13731–13767, 2014

ble 4) that the efficiency of gas-phase removal is sensitive to the volatility distribution of the organic matter. Shielding aged material from gas-phase removal (LOWVOL) lowers the average reductions of SOA concentration at the surface from −41/ − 56 % (aSOA/bSOA) to −32/ − 48 % vs. the NODEP case, and accelerating the aging process in general (FAST_AGING) further reduces the changes to −23/ − 39 %. Note that each of these changes is relative simulations where dry and wet deposition of SVOCs has been switched off, but which employs an otherwise identical VBS scheme (LOWVOL_NODEP and FAST_AGING_NODEP respectively). In all reductions except for anthropogenic organic matter in the FAST_AGING study, more mass is removed through the gas phase than through the particle phase. When looking at the resulting concentrations and their comparison against measurements (Fig. 5, bottom plot) we see that FAST_AGING exhibits a time evolution almost identical to the REF run, but shifted to higher concentrations. This leads to a strong overestimation during July and August. The concentrations predicted in the LOWVOL simulation lie in between REF and FAST_AGING. It is instructive to see that in LOWVOL, the variability of concentrations over the time period investigated is reduced. This actually resembles observations better, even though there is still a low bias in the mean. This suggests that VBS schemes currently used create a volatility distribution that is too volatile compared to the real atmosphere, although other effects may also be important.

5.2 Water solubility of SVOCs

Hodzic et al. (2014a) showed based on explicit oxidation chemistry modeling that good correlation exists between the volatility of a compound (C^*) and its water solubility (H^*). Still, uncertainy remains in the accuracy of these values, which is further amplified by the simplifications made in this work to apply them in a 3-D modeling context. This warrants an investigation of the sensitivity of our results to H^*. As a second motivation, the Wesely (1989) dry deposition parameterization used here is based on the analogue of a series of resistances, with Henry's law constants only affecting the canopy resistance. Once this resistance is sufficiently low (e.g. due to very high H^* values), the resulting

ACPD
14, 13731–13767, 2014

dry deposition velocities are only determined by the value of the other resistances. This would imply that above a certain value of H^*, dry deposition of SVOCs should not increase anymore and no additional reduction of SOA concentrations will occur. At which values of H^* exactly this saturation effect is observed in a realistic 3-D simulation was unknown. We hence conducted additional simulations with different values of H^* assigned to the volatility bins: 10^5, 10^8, and 10^{10} M atm^{-1}. In these simulations we ignore the temperature dependence of the Henry's law constants. Additionally we included a simulation using Henry's law values derived for HNO_3 ($H^* = 2.6 \times 10^6$ M atm^{-1}, $\mathrm{d}(\ln H^*)/\mathrm{d}(1/T) = 8700$), commonly used in models as reference for very soluble compounds for which exact H^* values are unknown. The resulting changes in average surface SOA concentrations and accumulated deposition (over the Continental US) are shown in Fig. 7. Results from the simulation using H^* values from explicit oxidation chemistry (REF) are included for reference. Changes in avg. SOA concentrations range from −25 % for $H^* = 10^5$ M atm^{-1} to −60 % for $H^* = 10^{10}$ M atm^{-1}. A saturation effect is visible between the simulations with H^* at 10^8 and 10^{10} M atm^{-1}, where resulting SOA concentrations change by less than 5 % despite changes in H^* of two orders of magnitude. This suggests that the effect of deposition of SVOCs has an upper limit of −60 % reduction in avg. surface SOA concentrations for the region and time period investigated here, corresponding roughly to Henry's law constants $> 10^{10}$ M atm^{-1}. It also shows that there is considerable variability in resulting SOA reductions within the range on H^* values used here, urging us to find ways to better constrain these removals to accurately describe the lifecycle of secondary organic aerosols. Note that these findings imply that, to be accurate, comparisons of SOA formation mechanisms implemented in 3-D models against measured concentrations will have to overestimate measured SOA concentrations by roughly 50 % if SVOC deposition is ignored (REF-NODEP), by 25 % if SVOC is deposited with $H^* = 10^5$ M atm^{-1} (REF-H_1E5), and still by 10–15 % (REF-H_HNO3) if dry and wet deposition of SVOCs is considered with H^* values of HNO_3.

ACPD
14, 13731–13767, 2014

5.3 Reactivity factor f_0

The Wesely (1989) dry deposition scheme considers the effect of chemical processing of reactive VOCs within plants by adding a reactivity factor f_0 to the calculation of mesophyll and leaf cuticular resistances. An f_0 of 0 represents unreactive substances, where as $f_0 = 1.0$ treats a species like O_3 (which immediately decomposes within the plant). In our work f_0 is set to 0.0, considering SVOCs to be unreactive. Karl et al. (2010) suggested based on flux measurements that oxidized organic trace gases should be considered reactive ($f_0 > 0$). To understand the effect of this treatment we conducted additional simulations where we set f_0 to 0.1 (F_0.1, slightly reactive) and 1.0 (F_1.0, reactive like O_3). We did not observe notable changes in the amount of deposited SVOCs and neither in the effect on SOA concentrations (not shown). This is reasoned by the fact that H^* values from GECKO used in our study are sufficiently high so that solubility dominates the mesophyll and cuticular resistances and the additional reduction in these resistances due to reactivity is negligible.

6 Conclusions

We investigated the effect of considering removal of semi-volatile organic compounds on secondary organic aerosols concentrations according to recent findings that suggest SVOCs are highly water soluble (Hodzic et al., 2014a). Simulations with the regional chemistry transport model WRF-Chem were conducted spanning the whole year 2010 over the domain of the continental US. Considering dry and wet deposition of SVOCs in the gas-phase with recently derived Henry's law constants reduces ground level SOA concentrations by 48 (aSOA)/63 (bSOA) in the annual average over the continental US in 2010. Dry deposition is much more effective than wet deposition, reducing surface level concentrations −40 vs. −8 % for aSOA and −52 vs. −11 % for bSOA. More than half of the total mass of SVOCs + SOA (61 % for anthropogenics, 76 % for biogenics) is actually deposited via the gas-phase. In a number of sensitivity

ACPD
14, 13731–13767, 2014

study spanning the months of June and July of 2010 we investigate the robustness of these findings by varying the volatility distribution of the organic matter, the Henry's law constants used, and the effect of the reactivity parameter f_0. We find that the efficiency of these removals is sensitive to the volatility of the mixture, reducing the resulting reductions in surface level SOA concentrations from −48 % (avg. of changes in aSOA and bSOA) in the standard simulation (REF) to −40 % when protecting aged SOA from gas-phase removal (LOWVOL), and to −31 % when accelerating the aging process in general (FAST_AGING). SOA is sensitive to the removal of SVOCs in the gas-phase through dry and wet deposition for the whole range of H^* values investigated, with average reductions in surface SOA concentrations of −25 % when assuming $H^* = 10^5\,\mathrm{M\,atm^{-1}}$, scaling up to −60 % for $H^* = 10^{10}\,\mathrm{M\,atm^{-1}}$. A saturation effect is clearly visible for $H^* \geq 10^8\,\mathrm{M\,atm^{-1}}$, suggesting that the upper bound of these processes on SOA concentrations is reached. Considering reactivity of SVOCs in the dry deposition calculation over vegetation as suggested by Karl et al. (2010) had no observable effect as the high values of water solubility calculated by GECKO dominate the calculation of the vegetation-related resistances.

Our findings have important implications for the aerosol modeling community, as they show that considering dry as well as wet deposition of SVOCs in the gas-phase is an essential part of accurately modeling SOA. Any evaluation of regional SOA modeling against observed concentrations of particulate organic matter is biased high about 50 % if SVOC removal is neglected completely, about 25 % if SVOC removal is considered with a Henry's law constant $H^* = 10^5\,\mathrm{M\,atm^{-1}}$, and still 10 % if the water solubility of HNO_3 is used. We also showed that the removal processes are still sensitive to the value of the Henry's law constant H^* used up to around $10^8\,\mathrm{M\,atm^{-1}}$. Including these processes suggests further that there is room for additional pathways (e.g. in-cloud, in-aerosol production) and precursors (evaporating POA, glyoxal) of SOA in order to close the gap with observations. We evaluated the modeling system against measurements of precipitation and wet deposition of inorganic ions, which lends confidence that the underlying processes are accurately captured. However, we are currently not able

ACPD
14, 13731–13767, 2014

to observationally constrain the organic carbon budget until a network of long-term, routine measurements of dry and wet deposition of organic matter is established.

Appendix A: Box model simulations

How efficient the removal of gas-phase SVOCs is in decreasing SOA concentrations depends directly on the amount of SVOCs created by the oxidation of precursors (vs. the production of very low volatility compounds that partition predominantly in the particle phase), and the time it takes for subsequent chemistry to decrease the compound's volatility enough so that it remains in the particle phase. In VBS terminology it is a function of the yields distribution and the "aging" rate constant kaging. To investigate these sensitivites we simulate chamber experiments in a box model, employing VBS-type parameterizations with different assumptions. In Figs. 8 and 9 we show the results of the oxidation of 1 ppbv α-pinene (kOH(α-pinene) = 5.2×10^{-11} cm^3 molec^{-1} s^{-1}) and toluene (kOH(toluene) = $1.7 \times 10^{-12} \times \exp(352/T)$ cm^3 molec^{-1} s^{-1}), assuming constant OH of 2.0×10^6 molec cc^{-1}, and subsequent formation of SOA using the yields of Lane et al. (2008b). Four different VBS parameterizations are presented: as described in Lane et al. (2008b) (LANE), as described as base case in this work (NODEP), a low-volatility sensitivity study used in this work that "protects" aged material by moving into an "inert" volatility bin (LOWVOL), and a sensitivity study where the accelerate the overall aging of SVOCs (FAST_AGING). In all parameterizations we assume that chemistry of later generation compounds further reduces their volatility, which is approximated by reducing SVOC volatility by a decade (1 bin) with an "aging" rate constant of kaging = 1×10^{-11} cm^3 molec^{-1} s^{-1}. In the LOWVOL sensitivity study, kaging from the bin with $C^* = 1.0$ to $C^* = 1.0 \times 10^{-4}$ is increased to 1×10^{-10} cm^3 molec^{-1} s^{-1}. In FAST_AGING, the aging rate constants for all bins are increased to 4×10^{-11} cm^3 molec^{-1} s^{-1}. A first-order loss (e-folding lifetime of 1 day) is applied to the vapor phase in all bins to simulate SVOC deposition. Temperature varies as sine function around 298 K with a 10 K amplitude and a wave-length of 24 h.

ACPD
14, 13731–13767, 2014

SOA formation from α-pinene peaks in the first hours of the simulation due to faster reaction with OH (Fig. 8, third row) and higher yields. After α-pinene is depleted, toluene provides addqitional condensable vapors mass almost throughout the 120 h simulated. Clearly visible from the volatility distributions after 24 h (Fig. 8, top row) is that in REF, LOWVOL, and especially in FAST_AGING, a substantial amount of mass is shifted into the particle phase due to aging into the "inert" bin at $C^* = 1 \times 10^{-4}$ compared to LANE. We compare these results to the thermodenuder experiments of Cappa and Jimenez (2010) where they find that the semi-volatile fraction of oxygenated organic aerosol (SV-OOA, Fig. 5f in Cappa and Jimenez, 2010) has 2/3 of the total mass (gas+particle) of compounds with $C^* \leq 2$ in the particle phase. It is evident that the three different parameterizations exhibit very different sensitivities to changes in temperature. LANE uses a relatively low enthalpy of vaporization (dH) of 30 kJ mol^{-1}, and consequently the total SOA mass (Fig. 8, second row) does not vary strongly. In the REF, LOWVOL and FAST_AGING parameterizations the higher dH of > 100 kJ mol^{-1} (parameterization of Epstein et al., 2009) are used, and these simulations intially react much stronger to changes in temperature. It is notable, however, that in the LOWVOL and FAST_AGING cases, temperature sensitivity quickly decreases and the result is almost completely insensitive to temperature after 72 h. This is obviously the result of moving mass more quickly into the "inert" bin (Fig. 9).

As the four parameterizations exhibit very different volatility distributions, application of a loss process to simulate SVOC deposition leads to very different total mass concentrations (Fig. 8, second row) and volatility distributions after 120 h (Fig. 9). While LANE only has 0.5 µg m^{-3} of SOA left (down from > 1 µg m^{-3} after 42 h), REF ends up with 2 µg m^{-3}, LOWVOL with almost 3 µg m^{-3}, and FAST_AGING with 5 µg m^{-3} of SOA after 120 h. The inert bin protects SOA mass from being depleted via equilibration with the gas-phase and subsequent removal through deposition. This effect is even stronger in the LOWVOL and FAST_AGING cases, as the overall exposure time (from initial formation to ending up in the inert bin) is shorter.

ACPD
14, 13731–13767, 2014

The Supplement related to this article is available online at doi:10.5194/acpd-14-13731-2014-supplement.

Acknowledgements. Sascha Madronich is thanked for fruitful discussions. We used data from the NADP network (National Atmospheric Deposition Program (NRSP-3) 2014. NADP Program Office, Illinois State Water Survey, 2204 Griffith, Champaign, IL 61820) and thank NADP for providing these. This research was supported by the National Center for Atmospheric Research, which is operated by the University Corporation for Atmospheric Research on behalf of the National Science Foundation, and by the DOE grant DE-SC0006711. Any opinions, findings and conclusions or recommendations expressed in the publication are those of the author(s) and do not necessarily reflect the views of the National Science Foundation. JLJ was supported by DOE (BER/ASR) DE-SC0006035, CARB 11-305, and NOAA NA13OAR4310063.

References

Ahmadov, R., McKeen, S., Robinson, A., Bahreini, R., Middlebrook, A., Gouw, J. D., Meagher, J., Hsie, E.-Y., Edgerton, E., Shaw, S., and Trainer, M.: A volatility basis set model for summertime secondary organic aerosols over the eastern United States in 2006, J. Geophys. Res.-Atmos., 117, D06301, doi:10.1029/2011JD016831, 2012. 13734, 13735, 13736

Aiken, A. C., DeCarlo, P. F., Kroll, J. H., Worsnop, D. R., Huffman, J. A., Docherty, K. S., Ulbrich, I. M., Mohr, C., Kimmel, J. R., Sueper, D., Sun, Y., Zhang, Q., Trimborn, A., Northway, M., Ziemann, P. J., Canagaratna, M. R., Onasch, T. B., Alfarra, M. R., Prevot, A., Dommen, J., Duplissy, J., Metzger, A., Baltensperger, U., and Jimenez, J. L.: O/C and OM/OC ratios of primary, secondary, and ambient organic aerosols with high-resolution time-of-flight aerosol mass spectrometry, Environ. Sci. Technol., 42, 4478–4485, 2008. 13741

Athanasopoulou, E., Vogel, H., Vogel, B., Tsimpidi, A. P., Pandis, S. N., Knote, C., and Fountoukis, C.: Modeling the meteorological and chemical effects of secondary organic aerosols during an EUCAARI campaign, Atmos. Chem. Phys., 13, 625–645, doi:10.5194/acp-13-625-2013, 2013. 13739

Aumont, B., Szopa, S., and Madronich, S.: Modelling the evolution of organic carbon during its gas-phase tropospheric oxidation: development of an explicit model based on a self gen-

ACPD
14, 13731–13767, 2014

erating approach, Atmos. Chem. Phys., 5, 2497–2517, doi:10.5194/acp-5-2497-2005, 2005. 13733, 13737
Bessagnet, B., Seigneur, C., and Menut, L.: Impact of dry deposition of semi-volatile organic compounds on secondary organic aerosols, Atmos. Environ., 44, 1781–1787, 2010. 13734
Cappa, C. D. and Jimenez, J. L.: Quantitative estimates of the volatility of ambient organic aerosol, Atmos. Chem. Phys., 10, 5409–5424, doi:10.5194/acp-10-5409-2010, 2010. 13733, 13743, 13749
Chapman, E. G., Gustafson Jr., W. I., Easter, R. C., Barnard, J. C., Ghan, S. J., Pekour, M. S., and Fast, J. D.: Coupling aerosol-cloud-radiative processes in the WRF-Chem model: Investigating the radiative impact of elevated point sources, Atmos. Chem. Phys., 9, 945–964, doi:10.5194/acp-9-945-2009, 2009. 13737
Computational and Information Systems Laboratory: Yellowstone: IBM iDataPlex System (NCAR Community Computing), available at: http://n2t.net/ark:/85065/d7wd3xhc (last access: April 2014), National Center for Atmospheric Research, Boulder, CO, 2012. 13738
Easter, R. C., Ghan, S. J., Zhang, Y., Saylor, R. D., Chapman, E. G., Laulainen, N. S., Abdul-Razzak, H., Leung, L. R., Bian, X., and Zaveri, R. A.: MIRAGE: model description and evaluation of aerosols and trace gases, J. Geophys. Res.-Atmos., 109, D20210, doi:10.1029/2004JD004571, 2004. 13737
Emmons, L. K., Walters, S., Hess, P. G., Lamarque, J.-F., Pfister, G. G., Fillmore, D., Granier, C., Guenther, A., Kinnison, D., Laepple, T., Orlando, J., Tie, X., Tyndall, G., Wiedinmyer, C., Baughcum, S. L., and Kloster, S.: Description and evaluation of the Model for Ozone and Related chemical Tracers, version 4 (MOZART-4), Geosci. Model Dev., 3, 43–67, doi:10.5194/gmd-3-43-2010, 2010. 13735
Epstein, S. A., Riipinen, I., and Donahue, N. M.: A semiempirical correlation between enthalpy of vaporization and saturation concentration for organic aerosol, Environ. Sci. Technol., 44, 743–748, 2009. 13736, 13749
Grell, G. A. and Dévényi, D.: A generalized approach to parameterizing convection combining ensemble and data assimilation techniques, Geophys. Res. Lett., 29, 38-1–38-4, doi:10.1029/2002GL015311, 2002. 13736
Hodzic, A., Madronich, S., Aumont, B., Lee-Taylor, J., Karl, T., Camredon, M., and Mouchel-Vallon, C.: Limited influence of dry deposition of semivolatile organic vapors on secondary organic aerosol formation in the urban plume, Geophys. Res. Lett., 40, 3302–3307, 2013. 13733

ACPD
14, 13731–13767, 2014

Hodzic, A., Aumont, B., Knote, C., Lee-Taylor, J., Madronich, S., and Tyndall, G.: Deposition of gas-phase organics as a loss of secondary organic aerosols: estimation of Henry's law constants and application to the Volatility Basis Set Algorithm, Geophys. Res. Lett., submitted, 2014a. 13733, 13734, 13737, 13738, 13744, 13746, 13756, 13757, 13765

Hodzic, A., Gochis D., Cui, Y., et al.: Meteorological conditions, emissions and transport of anthropogenic pollutants over the Central Rocky Mountains during the 2011 BEACHON-RoMBAS filed study, in preparation, 2014b.

Jimenez, J., Canagaratna, M., Donahue, N., Prevot, A., Zhang, Q., Kroll, J., DeCarlo, P., Allan, J., Coe, H., Ng, N., Aiken, A. C., Docherty, K. S., Ulbrich, I. M., Grieshop, A. P., Robinson, A. L., Duplissy, J., Smith, J. D., Wilson, K. R., Lanz, V. A., Hueglin, C., Sun, Y., Tian, J., Laaksonen, A., Raatikainen, T., Rautiainen, J., Vaattovaara, P., Ehn, M., Kulmala, M., Tomlinson, J. M., Collins, D. R., Cubison, M. J., Dunlea, E., Huffman, J. A., Onasch, T. B., Alfarra, M. R., Williams, P. I., Bower, K., Kondo, Y., Schneider, J., Drewnick, F., Borrmann, S., Weimer, S., Demerjian, K., Salcedo, D., Cottrell, L., Griffin, R. J., Takami, A., Miyoshi, T., Hatakeyama, S., Shimono, A., Sun, Y., Zhang, Y. M., Dzepina, K., Kimmel, J. R., Sueper, D., Jayne, J. T., Herndon, S. C., Trimborn, A., Williams, L., Wood, E. C., Middlebrook, A. M., Kolb, C. E., Baltensperger, U., and Worsnop, D. R.: Evolution of organic aerosols in the atmosphere, Science, 326, 1525–1529, 2009. 13733

Karl, T., Harley, P., Emmons, L., Thornton, B., Guenther, A., Basu, C., Turnipseed, A., and Jardine, K.: Efficient atmospheric cleansing of oxidized organic trace gases by vegetation, Science, 330, 816–819, 2010. 13739, 13746, 13747

Knote, C., Hodzic, A., Jimenez, J. L., Volkamer, R., Orlando, J. J., Baidar, S., Brioude, J., Fast, J., Gentner, D. R., Goldstein, A. H., Hayes, P. L., Knighton, W. B., Oetjen, H., Setyan, A., Stark, H., Thalman, R., Tyndall, G., Washenfelder, R., Waxman, E., and Zhang, Q.: Simulation of semi-explicit mechanisms of SOA formation from glyoxal in a 3-D model, Atmos. Chem. Phys. Discuss., 13, 26699–26759, doi:10.5194/acpd-13-26699-2013, 2013. 13735, 13742

Lane, T. E., Donahue, N. M., and Pandis, S. N.: Effect of NO_x on secondary organic aerosol concentrations, Environ. Sci. Technol., 42, 6022–6027, 2008a. 13735, 13736

Lane, T. E., Donahue, N. M., and Pandis, S. N.: Simulating secondary organic aerosol formation using the volatility basis-set approach in a chemical transport model, Atmos. Environ., 42, 7439–7451, 2008b. 13735, 13748

ACPD
14, 13731–13767, 2014

Lim, Y. B., Tan, Y., Perri, M. J., Seitzinger, S. P., and Turpin, B. J.: Aqueous chemistry and its role in secondary organic aerosol (SOA) formation, Atmos. Chem. Phys., 10, 10521–10539, doi:10.5194/acp-10-10521-2010, 2010. 13742

Murphy, B. N. and Pandis, S. N.: Simulating the formation of semivolatile primary and secondary organic aerosol in a regional chemical transport model, Environ. Sci. Technol., 43, 4722–4728, 2009. 13736

Murphy, D., Cziczo, D., Froyd, K., Hudson, P., Matthew, B., Middlebrook, A., Peltier, R. E., Sullivan, A., Thomson, D., and Weber, R.: Single-particle mass spectrometry of tropospheric aerosol particles, J. Geophys. Res.-Atmos., 111, D23S32, doi:10.1029/2006JD007340, 2006. 13733

National Centers for Environmental Prediction/National Weather Service/NOAA/US Department of Commerce: NCEP FNL Operational Model Global Tropospheric Analyses, continuing from July 1999, Research Data Archive at the National Center for Atmospheric Research, Computational and Information Systems Laboratory, Boulder, Colo. (updated daily), doi:10.5065/D6M043C6, 2000. 13738

Neu, J. L. and Prather, M. J.: Toward a more physical representation of precipitation scavenging in global chemistry models: cloud overlap and ice physics and their impact on tropospheric ozone, Atmos. Chem. Phys., 12, 3289–3310, doi:10.5194/acp-12-3289-2012, 2012. 13737

Odum, J. R., Hoffmann, T., Bowman, F., Collins, D., Flagan, R. C., and Seinfeld, J. H.: Gas/particle partitioning and secondary organic aerosol yields, Environ. Sci. Technol., 30, 2580–2585, 1996. 13733

Pankow, J. F.: An absorption model of gas/particle partitioning of organic compounds in the atmosphere, Atmos. Environ., 28, 185–188, 1994. 13733, 13736

Paulot, F., Crounse, J. D., Kjaergaard, H. G., Kürten, A., Clair, J. M. S., Seinfeld, J. H., and Wennberg, P. O.: Unexpected epoxide formation in the gas-phase photooxidation of isoprene, Science, 325, 730–733, 2009. 13742

Pye, H. O. T. and Seinfeld, J. H.: A global perspective on aerosol from low-volatility organic compounds, Atmos. Chem. Phys., 10, 4377–4401, doi:10.5194/acp-10-4377-2010, 2010. 13734

Rao, S. T., Galmarini, S., and Puckett, K.: Air Quality Model Evaluation International Initiative (AQMEII): advancing the state of the science in regional photochemical modeling and its applications, B. Am. Meteorol. Soc., 92, 23–30, 2011. 13738

ACPD
14, 13731–13767, 2014

Raventos-Duran, T., Camredon, M., Valorso, R., Mouchel-Vallon, C., and Aumont, B.: Structure-activity relationships to estimate the effective Henry's law constants of organics of atmospheric interest, Atmos. Chem. Phys., 10, 7643–7654, doi:10.5194/acp-10-7643-2010, 2010. 13733

Robinson, A. L., Donahue, N. M., Shrivastava, M. K., Weitkamp, E. A., Sage, A. M., Grieshop, A. P., Lane, T. E., Pierce, J. R., and Pandis, S. N.: Rethinking organic aerosols: semivolatile emissions and photochemical aging, Science, 315, 1259–1262, 2007. 13742

Shrivastava, M., Fast, J., Easter, R., Gustafson Jr., W. I., Zaveri, R. A., Jimenez, J. L., Saide, P., and Hodzic, A.: Modeling organic aerosols in a megacity: comparison of simple and complex representations of the volatility basis set approach, Atmos. Chem. Phys., 11, 6639–6662, doi:10.5194/acp-11-6639-2011, 2011. 13736

Stein, O., Flemming, J., Inness, A., Kaiser, J. W., and Schultz, M. G.: Global reactive gases forecasts and reanalysis in the MACC project, J. Int. Environ. Sci., 9, 57–70, 2012. 13738

Tsigaridis, K., Daskalakis, N., Kanakidou, M., Adams, P. J., Artaxo, P., Bahadur, R., Balkanski, Y., Bauer, S. E., Bellouin, N., Benedetti, A., Bergman, T., Berntsen, T. K., Beukes, J. P., Bian, H., Carslaw, K. S., Chin, M., Curci, G., Diehl, T., Easter, R. C., Ghan, S. J., Gong, S. L., Hodzic, A., Hoyle, C. R., Iversen, T., Jathar, S., Jimenez, J. L., Kaiser, J. W., Kirkevåg, A., Koch, D., Kokkola, H., Lee, Y. H., Lin, G., Liu, X., Luo, G., Ma, X., Mann, G. W., Mihalopoulos, N., Morcrette, J.-J., Müller, J.-F., Myhre, G., Myriokefalitakis, S., Ng, S., O'Donnell, D., Penner, J. E., Pozzoli, L., Pringle, K. J., Russell, L. M., Schulz, M., Sciare, J., Seland, Ø., Shindell, D. T., Sillman, S., Skeie, R. B., Spracklen, D., Stavrakou, T., Steenrod, S. D., Takemura, T., Tiitta, P., Tilmes, S., Tost, H., van Noije, T., van Zyl, P. G., von Salzen, K., Yu, F., Wang, Z., Wang, Z., Zaveri, R. A., Zhang, H., Zhang, K., Zhang, Q., and Zhang, X.: The AeroCom evaluation and intercomparison of organic aerosol in global models, Atmos. Chem. Phys. Discuss., 14, 6027–6161, doi:10.5194/acpd-14-6027-2014, 2014. 13733

Wesely, M.: Parameterization of surface resistances to gaseous dry deposition in regional-scale numerical models, Atmos. Environ., 23, 1293–1304, 1989. 13737, 13739, 13744, 13746, 13757

Zaveri, R. A., Easter, R. C., Fast, J. D., and Peters, L. K.: Model for simulating aerosol interactions and chemistry (MOSAIC), J. Geophys. Res.-Atmos., 113, D13204, doi:10.1029/2007JD008782, 2008. 13735

ACPD
14, 13731–13767, 2014

Table 1. Chosen parameterizations for selected physical processes in WRF.

Process	Parameterization
Radiation	RRTMG short- and longwave
Cloud microphysics	Morrison double-moment scheme
Land surface	Noah Land Surface Model
Urban surface	Urban Canopy Model
Planetary boundary layer	Mellor-Yamada Nakanishi and Niino 2.5
Cumulus parameterization	Grell 3-D ensemble

ACPD
14, 13731–13767, 2014

Table 2. Henry's law constants H^* ($M\,atm^{-1}$) for different volatility bins (C^* in $\mu g\,m^{-3}$, at 298 K) as derived in Hodzic et al. (2014a). Shown are averaged values used for anthropogenic and biogenic semi-volatile mixtures. All water solubilities are used with a temperature dependence of 6014 ($-d\ln(H^*)/d(1/T)$).

	1	10	100	1000
anthropogenic	1.1×10^8	1.8×10^7	3.2×10^6	5.5×10^5
biogenic	5.3×10^9	7.0×10^8	9.3×10^7	1.2×10^7

ACPD
14, 13731–13767, 2014

Table 3. Simulations conducted. DD/WD denotes if dry/wet deposition of SVOCs is considered, H^* refers to the Henry's law constants used for SVOCs, kOH to the aging rate constant (SVOC + OH), and f_0 to the reactivity parameter in the Wesely (1989) dry deposition scheme. kOH is reported as $cm^3\ molec^{-1}\ s^{-1}$, H^* as $M\ atm^{-1}$, the temperature dependence as $-d\ln(H^*)/d(1/T)$. Parameters varied compared to the REF simulation are shown in bold font.

case name	DD	WD	H^* (T dependence)	f_0	kOH
REF	x	x	Hodzic et al. (2014a)	0.0	1.0×10^{-11}
DRY	x		Hodzic et al. (2014a)	0.0	1.0×10^{-11}
WET		x	Hodzic et al. (2014a)	0.0	1.0×10^{-11}
NODEP			no SVOC deposition	0.0	1.0×10^{-11}
LOWVOL	x	x	Hodzic et al. (2014a)	0.0	1×10^{-11}, 1×10^{-10} for $C^* = 1.0$
LOWVOL_NODEP			no SVOC deposition	0.0	1×10^{-11}, 1×10^{-10} for $C^* = 1.0$
FAST_AGING	x	x	Hodzic et al. (2014a)	0.0	4.0×10^{-11}
FAST_AGING_NODEP			no SVOC deposition	0.0	4.0×10^{-11}
H_HNO3	x	x	2.6×10^6 (8700)	0.0	1.0×10^{-11}
H_1E5	x	x	1.0×10^5 (0)	0.0	1.0×10^{-11}
H_1E8	x	x	1.0×10^8 (0)	0.0	1.0×10^{-11}
H_1E10	x	x	1.0×10^{10} (0)	0.0	1.0×10^{-11}
F_0.1	x	x	Hodzic et al. (2014a)	0.1	1.0×10^{-11}
F_1.0	x	x	Hodzic et al. (2014a)	1.0	1.0×10^{-11}

ACPD
14, 13731–13767, 2014

Table 4. Contributions of dry and wet deposition through the gas-/particle-phase as well as resulting change in surface level SOA concentrations over the continental US in June, July, and August for the different VBS parameterizations considered. Values in the two lowermost rows are percentual changes (%), all other rows are accumulated deposited mass in Gg.

		REF		LOWVOL		FAST_AGING	
		anthro.	biog.	anthro.	biog.	anthro.	biog.
particle	wet dep.	21.9	19.4	15.5	13.7	32.7	31.8
	dry dep.	1.8	1.6	1.1	1.1	2.6	2.6
	total	23.7	21	16.6	14.8	35.3	34.4
gas	wet dep.	12.0	17.4	6.5	9.6	6.3	10.8
	dry dep.	21.5	42.9	11.1	25.2	12.3	30.4
	total	33.5	60.3	17.6	34.8	18.6	41.2
mass fraction lost by gas-phase dep. (%)		59	74	51	70	35	54
avg. surface SOA conc. changes (%)		−41	−56	−32	−48	−23	−39

ACPD
14, 13731–13767, 2014

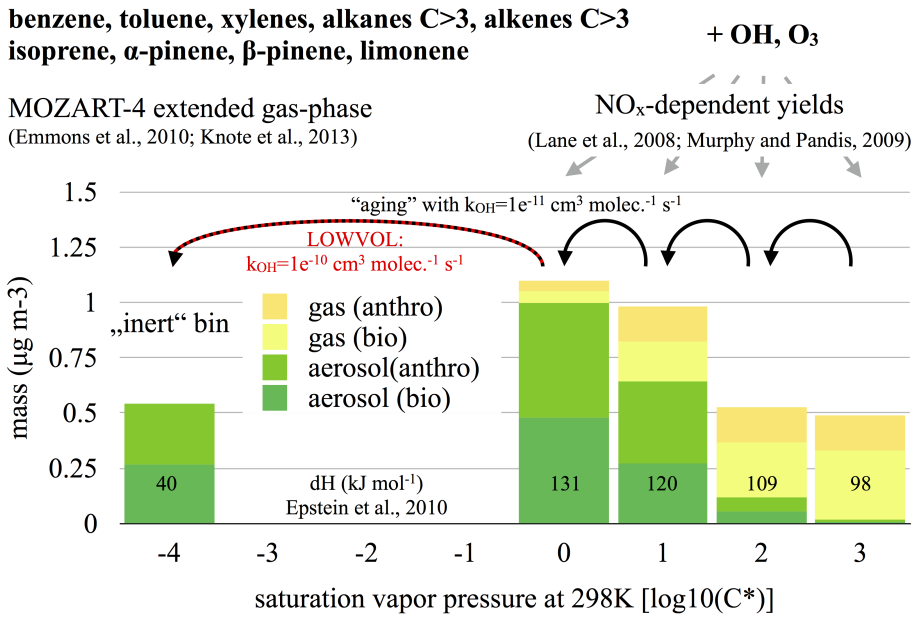

Figure 1. Schematic overview of the Volatility Basis Set as implemented in WRF-Chem. SOA/SVOC values are surface level concentrations from the REF simulation averaged over the full year 2010 and the CONUS domain (land points only).

ACPD
14, 13731–13767, 2014

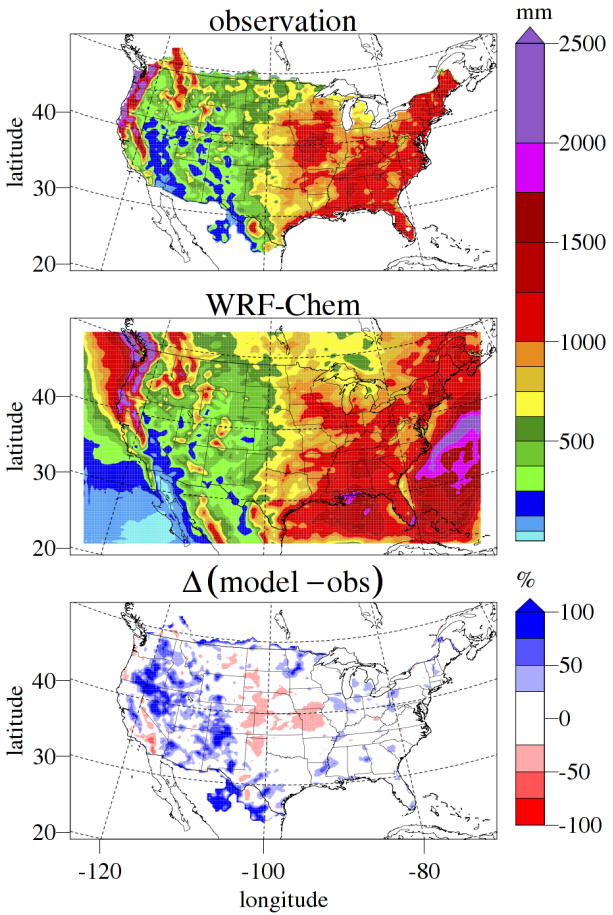

Figure 2. Year 2010 accumulated precipitation as observed by rain gauge/radar network (top left, "obs") vs. WRF-Chem model results (top right, "mod") and differences relative to the observations (bottom, Δ(model – obs) = (mod – obs)/obs × 100).

ACPD
14, 13731–13767, 2014

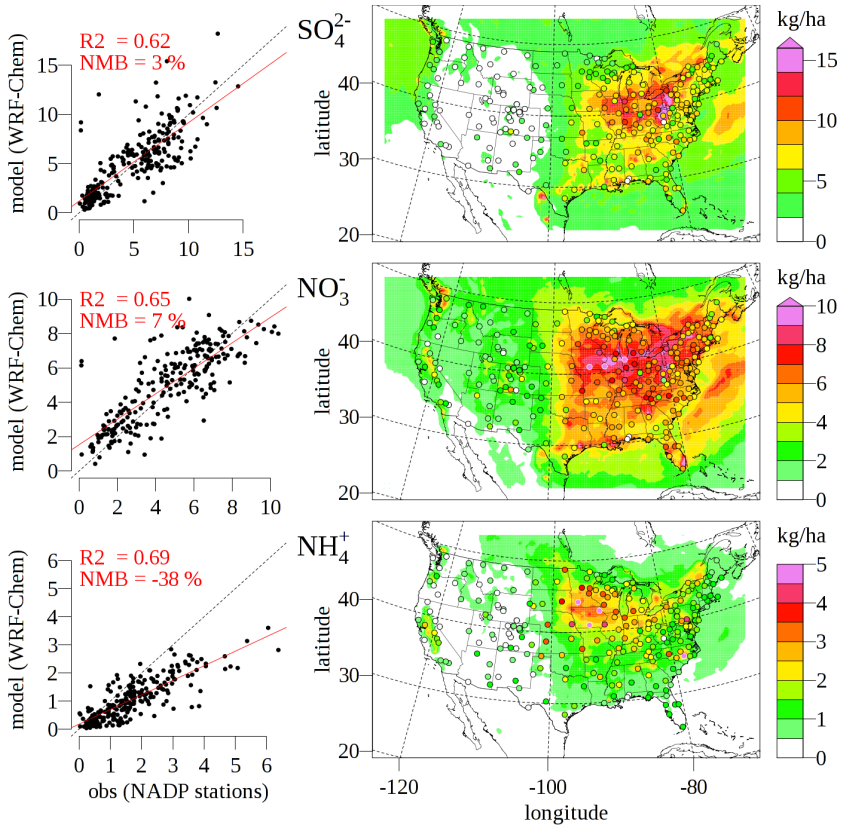

Figure 3. Year 2010 accumulated wet deposition of inorganic ions (SO_4^{2-}, NO_3^-, NH_4^+) as measured by NADP stations (obs) and as predicted by WRF-Chem (model). As maps (right column), with stations as circles color-coded by measured amount, and as scatterplots (left column) with R^2 the squared Pearson correlation coefficient, and NMB the normalized mean bias (NMB = Σ(model – obs)/Σobs × 100).

ACPD
14, 13731–13767, 2014

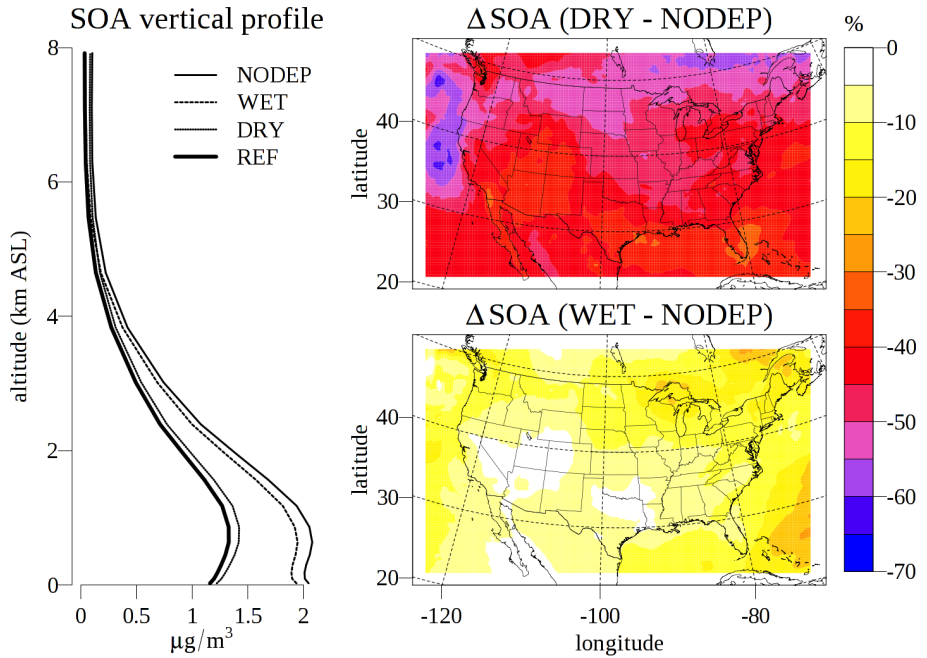

Figure 4. Effects of dry and wet deposition of SVOCs on SOA concentrations. Left plot: vertical profiles of SOA concentrations as yearly average over land. Right plots: changes in annual mean surface level SOA concentrations due to the consideration of dry (top, DRY – NODEP) and wet deposition (bottom, WET – NODEP) of SVOCs.

ACPD
14, 13731–13767, 2014

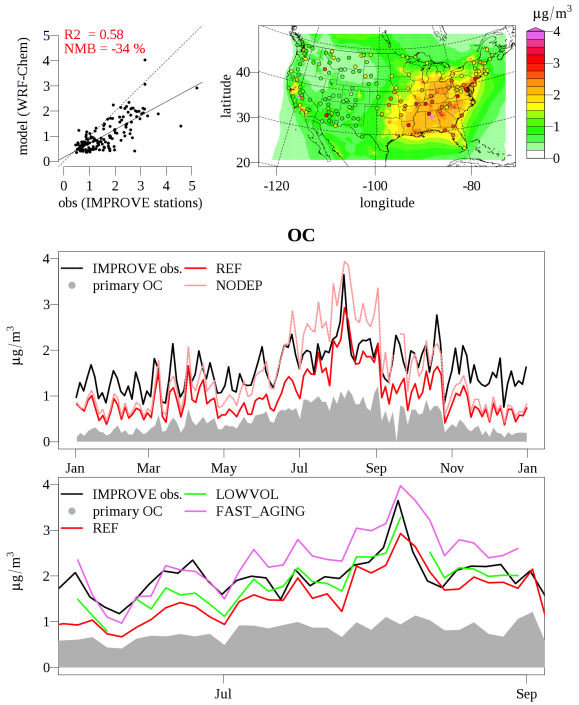

Figure 5. Evaluation of ground level total organic carbon (OC) concentrations against IMPROVE measurements. Top right: annual average OC surface level concentrations (REF simulation). Filled circles represent measured concentrations. Top left: scatterplot of annual average concentrations at each IMPROVE station against modeled concentrations (R^2 and NMB as defined in Fig. 3, again using the REF simulation). Lower plots: time evolution of OC concentrations as average over all IMPROVE stations. Black solid line is measurement average. Grey area represents the POC contribution to total OC (from REF simulation). Light red, red, green and violet lines are NODEP, REF, LOWVOL and FAST_AGING simulation averages of total OC respectively. The bottom plot shows only the summer period and adds sensitivity study results, but is otherwise identical to the middle plot.

ACPD
14, 13731–13767, 2014

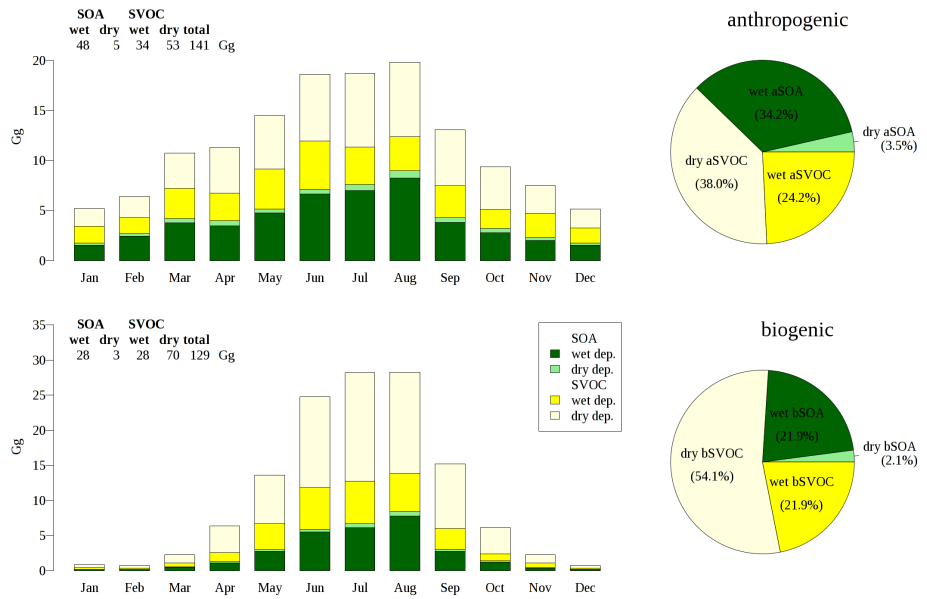

Figure 6. Monthly (left) and yearly (right) accumulated deposited mass of anthropogenic (top) and biogenic (bottom) SVOC + SOA over the continental US split into the different pathways, and shown (on the left) for simulations assuming H^* of SVOCs according to GECKO-A results (REF simulation). Table on top-left shows total annual deposited mass.

ACPD
14, 13731–13767, 2014

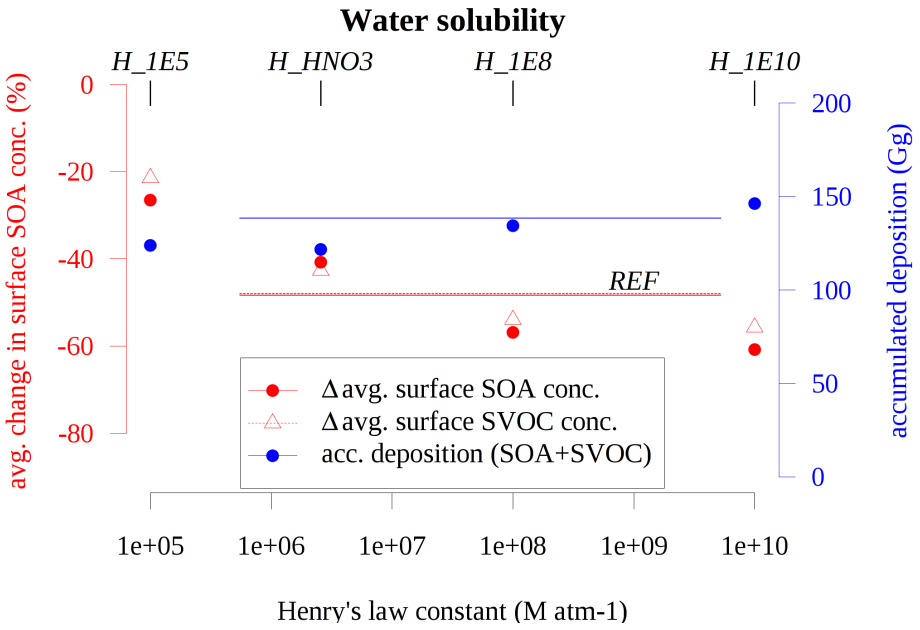

Figure 7. Sensitivity to water solubility of SVOCs (H^*). Shown are continental US averages/totals of changes in surface level SOA (red dots)/SVOC (red triangles) concentrations and accumulated deposition of SOA + SVOCs (blue dots). The results of the REF simulation using the range of H^* values derived in Hodzic et al. (2014a) are indicated as lines.

ACPD
14, 13731–13767, 2014

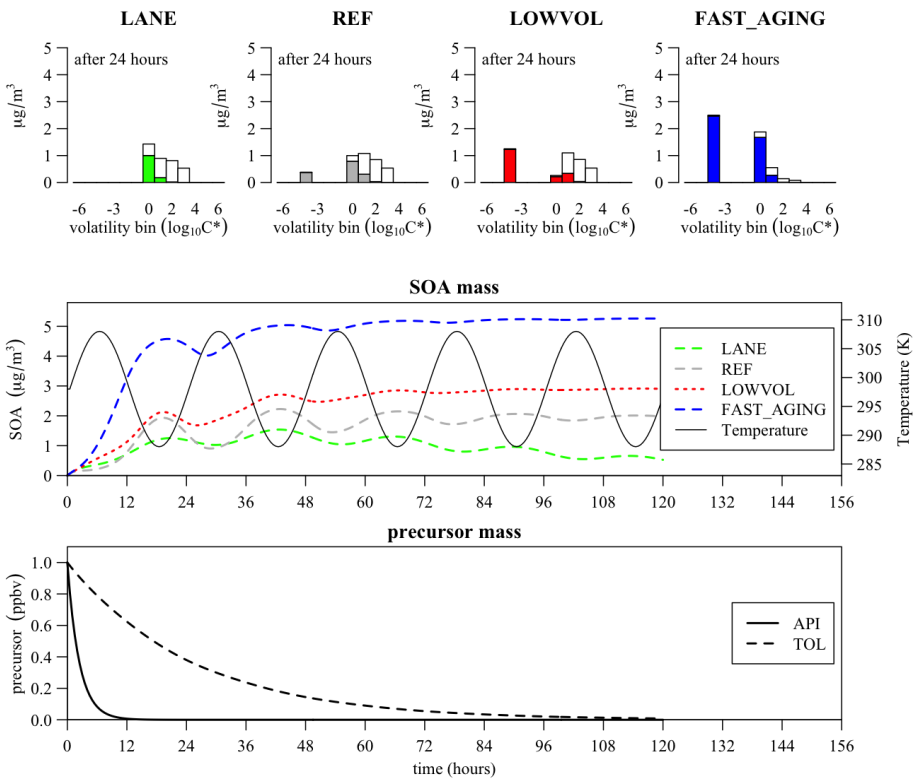

Figure 8. Box-model simulations of the oxidation of 1 ppbv α-pinene and toluene. Top row: distribution of particulate (colored) and vapor mass (white) in the different volatility bins after 24 h. Second row: total particle mass of SOA formed, as well as temperature. Third row: time evolution of precursor concentration.

ACPD
14, 13731–13767, 2014

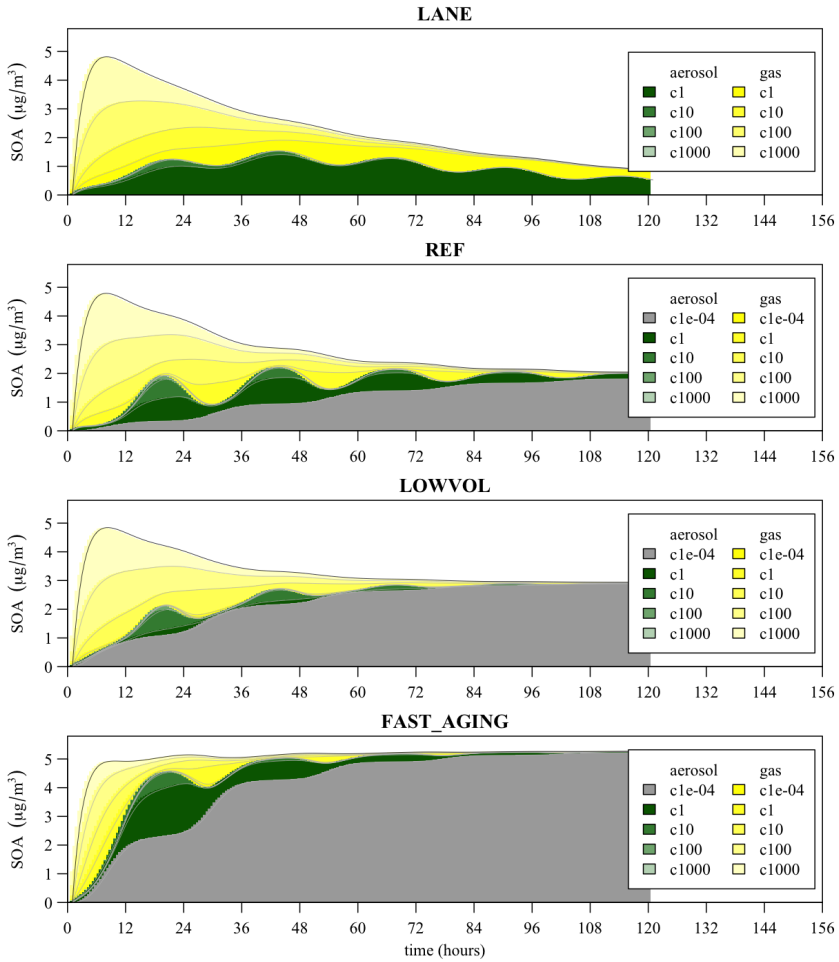

Figure 9. Evolution of mass distribution in particle and vapor phase in the box model simulations for the different parameterizations.

ACPD
14, 13731–13767, 2014